



REGULAR ARTICLE

Cyclopentadienyl iron dicarbonyl styrene chalcogenosulfonates: synthesis and structure of $\text{CpFe}(\text{CO})_2\text{SeSO}_2\text{CH}=\text{CHPh}$

MOHAMMAD EL-KHATEEB^{a,*}, ALAA AL-MOMANI^a, PILAR GARCIA-ORDUNA^b and FERNANDO J LAHOZ^b

^aChemistry Department, Jordan University of Science and Technology, Irbid 22110, Jordan

^bInorganic Chemistry Department, Institute for Chemical Synthesis and Homogeneous Catalysis, CSIC – University of Zaragoza, 50009 Zaragoza, Spain

E-mail: kateeb@just.edu.jo; mpgaor@unizar.es

MS received 28 August 2021; revised 14 October 2021; accepted 18 October 2021

Abstract. In this contribution, we report the preparation of iron thiosulfonato complex $\text{CpFe}(\text{CO})_2\text{SSO}_2\text{CH}=\text{CHPh}$ (**1**) and its selenosulfonato analogue $\text{CpFe}(\text{CO})_2\text{SeSO}_2\text{CH}=\text{CHPh}$ (**2**) featuring styrene moiety. **1** and **2** are obtained by electrophilic attack of $(\mu\text{-E}_x)[\text{CpFe}(\text{CO})_2]_2$ ($\text{E} = \text{S}$; $x = 2\text{--}4$, $\text{E} = \text{Se}$; $x = 1$) on the sulfur atom of styrene sulfonyl chloride $\text{ClSO}_2\text{CH}=\text{CHPh}$. The new compounds, **1** and **2** have been characterized by elemental analyses, IR, ^1H -, $^{13}\text{C}\{^1\text{H}\}$ -NMR, UV–Vis spectroscopy and the structure of **2** is determined by X-ray crystallography.

Keywords. Iron; Chalcogen; Styrene chalcogenosulfonate; X-ray structure; Characterization.

1. Introduction

Iron complexes incorporating sulfur or selenium ligands stimulate increasing interest due to their importance in biological systems,^{1–4} their relevance to catalytic processes^{5–9} and in the development of material science.^{10–13} Iron-sulfur proteins are required for many biological processes. They are involved in numerous cellular processes like respiration, photosynthesis, metabolic reactions, nitrogen fixation, DNA replication and repair, regulation of gene expression or t-RNA modifications.^{1–4} The influence of the incorporation of sulfur or selenium atoms into the structure of [FeFe]-hydrogenase models, has been investigated on their activity for hydrogen production.^{5–9} Iron sulfide nanomaterials have been used as electrocatalysts for water-splitting leading to hydrogen evolution.¹² Iron selenocarboxylates show antifungal, antibacterial effects and are active substrates against cancer cells.^{14,15}

In the past two decades, we have developed a synthetic methodology for iron complexes of the general formula $\text{CpFe}(\text{CO})_2\text{EQ}$ ($\text{E} = \text{S}, \text{Se}$, $\text{Q} = \text{COR}$,^{16,17}

SO_2R ,^{18,19} COCO_2R ,²⁰ CO_2R ,^{21,22} $\text{C}(\text{S})\text{OR}$,^{23,24} $\text{C}(\text{O})\text{SR}$,^{25,26} CS_2R ²⁷). This methodology involves the interaction of iron sulfides or selenide bridged dimers $(\mu\text{-E}_x)[\text{CpFe}(\text{CO})_2]_2$ ($\text{E} = \text{S}$, $x = 2\text{--}4$; $\text{E} = \text{Se}$, $x = 1$) with the corresponding chlorides (QCl).^{16–27} The dicarbonyl complexes underwent photolytic substitution with AR_3 to give the substituted products $\text{CpFe}(\text{CO})(\text{AR}_3)\text{EQ}$ ($\text{A} = \text{P}$; $\text{R} = \text{OEt}, \text{Ph}$, $\text{A} = \text{As}, \text{Sb}$; $\text{R} = \text{Ph}$).^{28–31} For bis(diphenylphosphino)alkanes (dppa), the photolytic reactions of $\text{CpFe}(\text{CO})_2\text{SCOR}$ gave the mono-substituted complexes $\text{CpFe}(\text{CO})(\kappa\text{P-dppa})\text{SCOR}$ or the disubstituted ones $\text{CpFe}(\kappa^2\text{P,P-dppa})\text{SCOR}$ depending on the reaction conditions.^{32,33}

Thiosulfonato iron complexes represent an important class of complexes that model the Claus process in which the sulfur-sulfur bond formation is a key step. To that end, the iron thiosulfonates $\text{CpFe}(\text{CO})_2\text{SSO}_2\text{R}$ ($\text{R} = \text{CF}_3, \text{CCl}_3, \text{C}_6\text{F}_5$)¹⁸ and their corresponding selenosulfonate $\text{CpFe}(\text{CO})_2\text{SeSO}_2\text{R}$ ($\text{R} = \text{Me}, \text{Ph}, 4\text{-C}_6\text{H}_4\text{Cl}, 4\text{-C}_6\text{H}_4\text{Me}$) have been reported.¹⁹ The analogous heterocyclic complexes $\text{CpFe}(\text{CO})_2\text{ESO}_2\text{-het}$ ($\text{het} = 2\text{-C}_4\text{H}_3\text{S}, 5\text{-C}_4\text{H}_2\text{SCl}$) are reported from the

*For correspondence

Supplementary Information: The online version contains supplementary material available at <https://doi.org/10.1007/s12039-021-02012-2>.

chalcogenide dimers and the heterocyclic sulfonyl chlorides.³⁴ Monomeric $\text{CpFe}(\text{CO})_2\text{ESO}_2\text{-1,3-C}_6\text{H}_4\text{SO}_2\text{Cl}$ and dimeric chalcogenosulfonates $\text{CpFe}(\text{CO})_2\text{ESO}_2\text{-1,3-C}_6\text{H}_4\text{SO}_2\text{EFe}(\text{CO})_2\text{Cp}$ may also be obtained by varying the chalcogenide to disulfonyl chloride ratio.³⁴

Thiosulfonato complexes for ruthenium are accessible from the reaction of the hydrogensulfido complexes $\text{CpRu}(\text{dppa})\text{SH}$ with sulfonyl chlorides.³⁵ In an analogous synthesis, the reaction of $\text{CpW}(\text{CO})_3\text{SH}$ with sulfonyl chlorides generated the tungsten thiosulfonato complexes $\text{CpW}(\text{CO})_3\text{SSO}_2\text{R}$.³⁶ However, the corresponding tungsten selenosulfonato complexes are produced from the reaction of the anion $\text{CpW}(\text{CO})_3\text{Se}^-$ with sulfonyl chlorides.³⁷

In continuation of our work on the area of organoiron chalcogen complexes, this paper describes the synthesis of thio- and selenosulfonates bearing a particular styrene moiety. The X-ray structure of $\text{CpFe}(\text{CO})_2\text{SeSO}_2\text{CH=CHPh}$ is presented.

2. Experimental

2.1 Materials and methods

Synthesis and manipulations were performed under an atmosphere of nitrogen using standard Schlenk techniques. Diethyl ether and hexane were dried over sodium/benzophenone and CH_2Cl_2 was dried over P_2O_5 following standard procedures. The reagents $[\text{CpFe}(\text{CO})_2]_2$, sulfur, selenium, styrene sulfonyl chloride (Aldrich) were used as received. The complexes $(\mu\text{-Se})[\text{CpFe}(\text{CO})_2]_2$ and $(\mu\text{-S}_x)[\text{CpFe}(\text{CO})_2]_2$ ($x = 2\text{-}4$) were prepared by literature methods.^{38,39} Bruker-Avance 400 MHz spectrometer was used to measure the nuclear magnetic resonance (NMR) spectra of the synthesized complexes. Chemical shifts are in ppm relative to TMS at 0 ppm (^1H) and to CDCl_3 peak (^{13}C). Melting points were measured on an electrothermal melting point apparatus and are uncorrected. Elemental analyses were performed using a vairo EL III CHNS (Elemental analyse GmbH Hanau) as single determination. The UV-Vis and IR spectra were recorded with a Shimadzu 240-UV-Vis and a Bruker alpha FT-IR spectrometer equipped with ATR unit, respectively.

2.2 General procedure for the preparation of $\text{CpFe}(\text{CO})_2\text{ESO}_2\text{CH=CHPh}$ ($E = \text{S}$ (1), Se (2))

A Schlenk flask was charged with the iron chalcogenides $(\mu\text{-E}_x)[\text{CpFe}(\text{CO})_2]_2$ (2.83 mmol) in 100 mL

of diethyl ether. Styrene sulfonyl chloride (0.59 g, 2.90 mmol) dissolved in 20 mL of diethyl ether was added dropwise to the iron chalcogenide solution. The resulting mixture was stirred at room temperature until the reaction is complete as shown by TLC (~ 48 h). The volatiles were removed under vacuum and the remaining solid was dissolved in 2 mL of CH_2Cl_2 and was introduced to a silica gel column made up of hexane. Elution with a mixture of dichloromethane and hexane (1:1 volume ratio) gave an orange band which was collected and identified as $\text{CpFe}(\text{CO})_2\text{ESO}_2\text{CH=CHPh}$ followed by a red band which was also collected and identified as $\text{CpFe}(\text{CO})_2\text{Cl}$ with about 40% isolated yield. The products $\text{CpFe}(\text{CO})_2\text{ESO}_2\text{CH=CHPh}$ were recrystallized from $\text{CH}_2\text{Cl}_2/\text{hexane}$ at -4 °C.

2.2.1. $\text{CpFe}(\text{CO})_2\text{SSO}_2\text{CH=CHPh}$ (1) Orange (75%). M.p.: 146-147 °C. IR (cm^{-1}): $\nu_{\text{C}\equiv\text{O}}$ 2030 (s), 1972 (s); $\nu_{\text{C}=\text{C}}$ 1656 (m), ν_{SO_2} 1273 (s), 1100 (s). $^1\text{H-NMR}$ (CDCl_3) δ : 5.23 (s, 5H, Cp); 7.01 (d, 1H, SO_2CH); 7.37 (m, 5H, Ph); 7.46 (d, 1H, CH-Ph). $^{13}\text{C}\{^1\text{H}\}\text{-NMR}$ (CDCl_3) δ : 85.81 (Cp), 129.16, 129.50, 130.71 (Ph), 134.71, 137.26 (C=C), 211.74 (CO). UV-Vis (CH_2Cl_2 : λ_{max} (nm): 293, 330. Anal. Calc. for $\text{C}_{15}\text{H}_{12}\text{FeO}_4\text{S}_2$: C, 47.88; H, 3.20; S, 17.04%. Found: C, 47.43; H, 3.10; S, 16.42%.

2.2.2. $\text{CpFe}(\text{CO})_2\text{SeSO}_2\text{CH=CHPh}$ (2) Dark brown (80%). M.p.: 140-141 °C. IR (cm^{-1}): $\nu_{\text{C}\equiv\text{O}}$ 2046 (s), 1996 (s); $\nu_{\text{C}=\text{C}}$ 1660 (m); ν_{SO_2} 1263 (s), 1098 (s). $^1\text{H-NMR}$ (CDCl_3) δ : 5.28 (s, 5H, Cp); 7.06 (d, 1H, SO_2CH); 7.38 (m, 5H, Ph); 7.46 (d, 1H, CH-Ph). $^{13}\text{C}\{^1\text{H}\}\text{-NMR}$ (CDCl_3) δ : 86.21 (Cp), 128.55, 129.24, 130.51 (Ph), 133.98, 137.76 (C=C), 210.82 (CO). $^{77}\text{Se}\{^1\text{H}\}\text{-NMR}$ (CDCl_3) δ : 429.91. UV-Vis (CH_2Cl_2 : λ_{max} (nm): 286, 337. Anal. Calc. for $\text{C}_{15}\text{H}_{12}\text{FeO}_4\text{SSe}$: C, 42.58; H, 2.86%. Found: C, 42.17; H, 2.74 %.

2.3 Crystal structure determination of 2

Single crystal X-ray diffraction data were collected on a Smart Apex Bruker diffractometer, using graphite-monochromated Mo-K_α radiation. The selected crystal was mounted on a fibre, coated with protecting perfluoropolyether oil and cooled to 100(2) K with an open-flow nitrogen gas chiller. Data were collected using ω scans with narrow oscillation frame strategy ($\Delta\omega = 0.3^\circ$), at several ϕ angles. Data were integrated and corrected for Lorentz, polarization and absorption effects with SAINT⁴⁰ and SADABS⁴¹ programs, integrated in APEX3 package. The structure was

solved by direct methods (SHELXS)⁴² and refined by full-matrix least squares techniques against F^2 (SHELXL),⁴³ included in WingX package.⁴⁴ All hydrogen atoms were found in difference Fourier maps, included in the model at observed positions and freely refined.

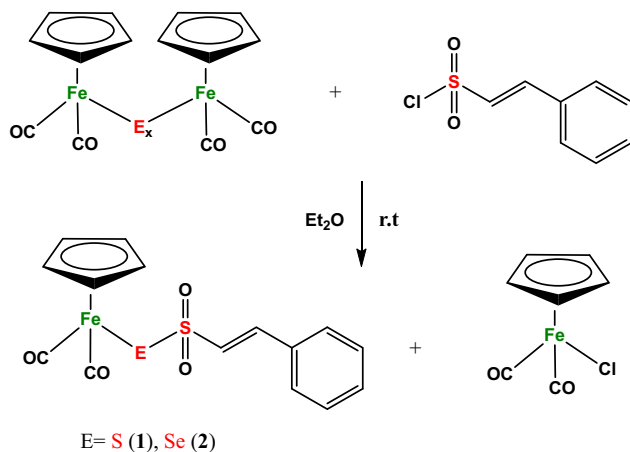
2.3.1 Crystallographic Data for 2: $C_{15}H_{12}FeO_4SSe$, Mr 423.12 g mol⁻¹, intense orange prism, size 0.080 × 0.110 × 0.230 mm³, monoclinic, space group $P2_1/c$, $a = 15.9886(10)$, $b = 5.9217(4)$, $c = 17.0603(10)$ Å, $\beta = 103.89(10)$, $V = 1568.03(17)$ Å³, $T = 100(2)$ K, $Z = 4$, $\mu = 3.429$ mm⁻¹, min and max transmission factors: 0.6067 and 0.7565; $F(000) = 840$, 24537 reflections measured in the range $2.460 < \theta < 28.382^\circ$ (completeness to θ_{max} 98.4%), 24537/3855 collected/independent reflections, $R_{int} = 0.0365$, number of data/restraint/parameters 3855/0/247, $R_1 = 0.0307$, $wR_2 = 0.0679$ [3379 reflections, $I > 2\sigma(I)$], $R_2 = 0.0388$, $wR_2 = 0.0720$, $GOOF = 1.041$ (all reflections), largest difference peak and hole: 1.071 / -0.555 (e/Å³).

3. Results and Discussion

3.1 Synthesis

The iron chalcogenosulfonato complexes $\{CpFe(CO)_2SSO_2CH=CHPh$ (**1**) or $CpFe(CO)_2SeSO_2CH=CHPh$ (**2**) were produced by the reaction of the iron sulfides or selenide with the styrene sulfonyl chloride in diethyl ether at room temperature as shown in Scheme 1.

A plausible mechanism for the reaction of the iron trisulfide dimer (as an example) with the sulfonyl chloride is shown in Scheme 2. The reactivity of the sulfide dimer towards sulfonyl chloride as electrophile is attributed to the presence of electron pairs on the bridging sulfur atoms.

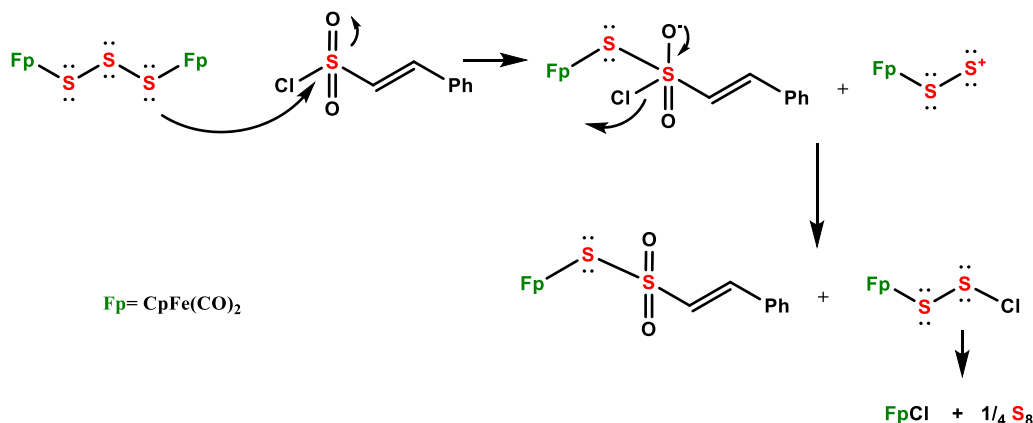


Scheme 1. Synthesis of iron chalcogenosulfonato complexes **1** and **2**.

The two new complexes (**1** and **2**) are air-stable as solids and air-sensitive in solution. These complexes are soluble in THF, diethyl ether and CH_2Cl_2 but insoluble in hydrocarbons. They have been characterized based on their IR, ¹H-, ¹³C{¹H}-NMR spectroscopy and by a single-crystal X-ray structure determination of **2**. Their IR spectra exhibited two strong bands of the terminal carbonyls (**1**: 1972, 2030 and **2**: 1996, 2046 cm⁻¹). The bands of **2** are found at higher frequency compared to those of **1** due to stronger σ -donor ability of the selenosulfonato group compared to the thiosulfonato. A similar shift has been observed for the analogous thio-/selenosulfonato systems.^{18,19} The sulfonato group displayed its presence by the symmetric and asymmetric stretching frequencies (**1**: 1100, 1273, **2**: 1098, 1263 cm⁻¹). These bands are within the same range observed for alkyl or aryl thio- or selenosulfonato analogs.^{18,19,36–38} The C=C frequency of these complexes (1656, 1660 cm⁻¹) is higher than the corresponding frequency of $CpFe(CO)_2SCOCH=CR_2$ (1619–1622 cm⁻¹)⁴⁵ and that for $CpFe(CO)_2SeCOCH=CR_2$ (1637–1649 cm⁻¹).¹⁷ This difference may be attributed to more resonance between the C=O and C=C bonds in the latter complexes. The ¹H NMR spectra of **1** and **2** exhibited singlet peak at 5.20 and 5.28 ppm for the Cp-protons, respectively. This resonance is within the same range reported for thio- and selenosulfonates (5.19–5.28).^{18,19} The ¹³C{¹H} NMR spectra of complexes **1** and **2** showed a downfield peak at 210.82 or 211.74 ppm for the carbonyl carbons and the peak at 85.81 or 86.21 ppm is due to the carbons of the Cp rings, respectively. The phenyl protons for both complexes are found in the range of 128.55–130.71 ppm while the peaks in range of 133.98–137.76 ppm are due to the vinylic carbon atoms. These ranges are similar to those observed for vinylic thio- and selenocarboxylato analogues.^{17,40} The ⁷⁷Se-NMR spectrum of $CpFe(CO)_2SeSO_2CH=CHC_6H_5$ has a singlet peak at 492.91 ppm for the Se atom present in this complex. This peak is higher than that reported for $CpFe(CO)_2SeCOCH=CR_2$ (188.70–190.01 ppm).¹⁷

3.2 Crystal structure of $CpFe(CO)_2SeSO_2CH=CHPh$ (**2**)

The molecular structure of complex **2**, determined by X-ray crystallography, is depicted in Figure 1. Selected geometrical parameters are reported in Table 1. The complex adopts a three-legged piano-stool



Scheme 2. A possible mechanism for the reaction of iron sulfide dimer with styrene sulfonyl chloride.

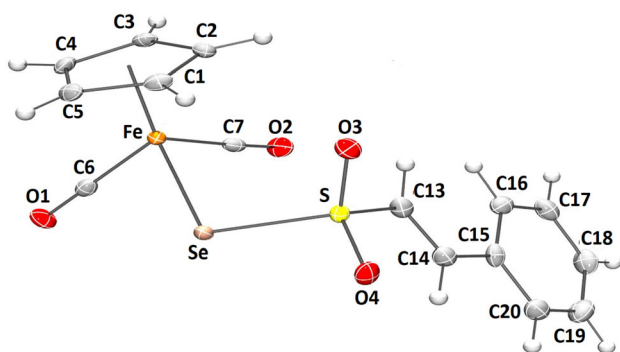


Figure 1. Molecular structure of CpFe(CO)₂SeSO₂-CH=CHPh (**2**).

Table 1. Selected bond lengths (Å) and angles (°) for complex **2**.

Fe-Se	2.3926(4)	Se-Fe-Ct ^a	123.85(4)
Fe-Ct ^a	1.7215(13)	Se-Fe-C6	86.96(8)
Fe-Se	2.3926(4)	Se-Fe-C7	93.70(8)
Fe-Ct ^a	1.7215(13)	Ct ^a -Fe-C6	124.99(10)
Fe-C6	1.785(3)	Ct ^a -Fe-C7	124.12(9)
Fe-C7	1.774(3)	C6-Fe-C7	93.13(12)
Fe-C1	2.128(3)	Fe-Se-S	107.04(2)
Fe-C2	2.105(3)	Se-S-3O	111.46(8)
Fe-C3	2.091(3)	Se-S-4O	105.27(9)
Fe-C4	2.098(3)	Se-S-13C	107.31(9)
Fe-C5	2.105(3)	3O-S-4O	118.38(13)
Se-S	2.2094(6)	O3-S-13C	104.77(14)
S-3O	1.444(2)	4O-S-13C	109.23(13)
S-4O	1.442(2)		
S-C13	1.764(3)		
C13-C14	1.321(4)		

^aCt represents the centroid of the Cp ligand.

geometry with iron coordinated to an η^5 -C₅H₅ group, to the two carbons of the carbonyl groups and to the selenium atom. The Fe-C(Cp) distances (2.091(3)-2.128(3) Å) and the Fe-C(CO) bond lengths (1.785(3), 1.774(3) Å) are identical to those of the closely related

selenosulfonato complex CpFe(CO)₂SeSO₂Ph¹⁹ and comparable to those of the selenocarboxylato complex CpFe(CO)₂SeCOCH=CMe₂ (mean values Fe-C(Cp) 2.091 Å, and Fe-C(CO) 1.771(2) Å)¹⁷ indicating a similar electron density around the iron center. Compared to other CpFe(CO)₂SeQ complexes, the Fe-Se bond length of 2.3926(4) Å nicely agrees with that of CpFe(CO)₂SeSO₂Ph (2.394(3) Å)¹⁹ and it is slightly longer than that of selenocarboxylato related complex, CpFe(CO)₂SeCOCH=CMe₂ (2.3844(4) Å).¹⁷

The iron coordination sphere adopts a pseudo-octahedral environment with the Cp-ligand formally occupying three coordination sites. The structure may be described as pseudo-octahedral rather than pseudo-tetrahedral, as the bond angles between monodentate ligands (Se-Fe-C angles: 86.96 and 93.70(8)°, and C-Fe-C angle of 93.13(12)°) are close to 90°, whereas the bond angles defined by the ring centroid, the Fe atom and the other ligands are *ca.* 124°. The S-Se (2.2094(6) Å) and S-O (1.442 and 1.444(3) Å) bond lengths of the selenosulfonato group are comparable to those reported for a similar system.^{17,19,40} The Se and S atoms are both sp³ hybridized as proved by the Fe-Se-S (107.04(2)°) and the S bond angles (mean value: 109.40(4)°).

It is noteworthy that the selenium atom is involved in a quite directional hydrogen bond interaction along the **b** axis. Selenium (or sulfur) atoms have lower electronegativity than oxygen, nitrogen or halogen atoms, and therefore they have been considered as poor H-bond acceptors. However, recent results pointed out their versatility in molecular assemblies, structural biology and functional materials.⁴⁶ Geometrical parameters describing this interaction of complex **2** (Figure 2), together with those of two classical C-H...O hydrogen bonds are reported in Table 2.

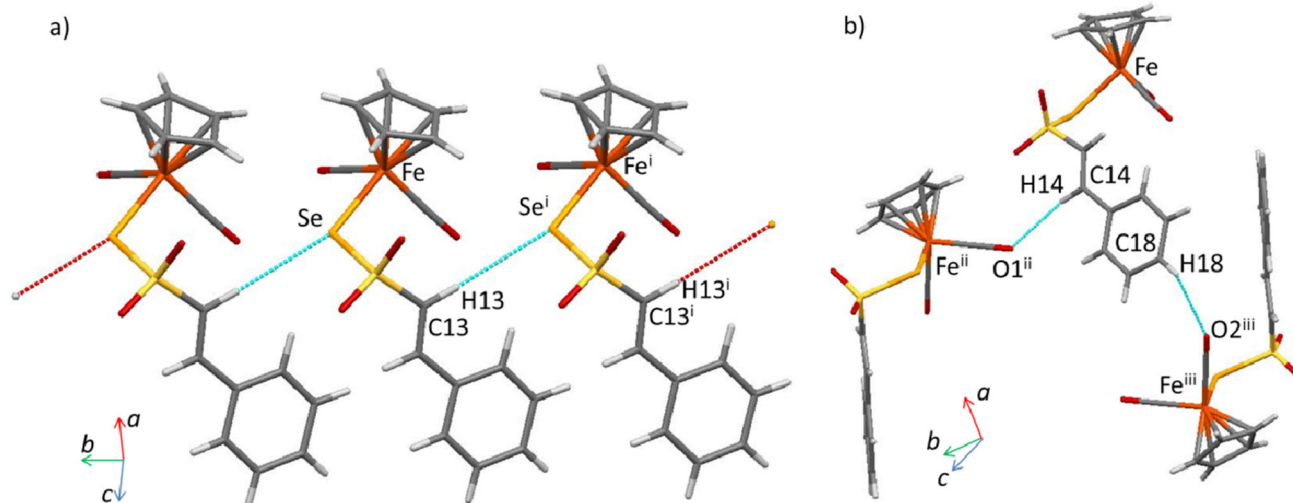


Figure 2. Hydrogen bond intermolecular interactions in complex **2**. (a) H-bonding involving Se atom. (b) H-bonding involving carbonylic oxygens. Symmetry codes: i) $x, -1+y, z$ ii) $x, -y+1/2, z+1/2$ iii) $1-x, -1/2 +y, 3/2-z$.

Table 2. Geometrical parameters (\AA , $^\circ$) of hydrogen bond intermolecular interactions in complex **2**.

D-H...A	D-H	H...A	D...A	D-H...A
C13-H13...Se ⁱ	1.01(4)	3.02(4)	4.031(2)	173(3)
C14-H14...O1 ⁱⁱ	1.01(4)	2.50(4)	3.439(3)	155(3)
C18-H18...O2 ⁱⁱⁱ	0.90(3)	2.57(3)	3.417(4)	156(3)

Symmetry codes: i) $x, -1+y, z$ ii) $x, -y+1/2, z+1/2$ iii) $1-x, -1/2 +y, 3/2-z$

3.3 UV-Vis spectra of complexes 1 and 2

The absorption spectra of complexes **1** and **2** were recorded in dichloromethane. UV-Vis spectroscopy is measured to show the types of electronic transitions occur within complexes **1** and **2**. A change in electron distribution between the metal and the ligand gives rise to charge transfer (CT) bands. For ligands having (σ , σ^* , π , π^* , n) molecular orbitals, charge transfer may occur from the ligand molecular orbitals to the metal d-orbitals (LMCT). However, if the metal is in a low oxidation state and the ligand has low-lying empty orbitals then a metal-to-ligand charge transfer (MLCT) may occur.⁴⁷ The spectrum of each complex showed two absorption bands; the high energy bands at 293 (**1**) and 286 (**2**) nm have been assigned as ligand–ligand charge transfer (LLCT) type, while the second bands (**1**: 330, **2**: 337 nm) were attributed to the Fe-Cp MLCT. Another very weak band around 450 nm is observed and may be attributed to an iron d-d transition. These bands have been assigned relative to/in agreement with analogous reported systems.^{17,18,25,26}

4. Conclusions

In conclusion, we have presented the synthesis and characterization of two iron chalcogenosulfonato complexes bearing styrene moiety in order to understand the role of the carbon-carbon double bond on the reactivity of the styrene sulfonyl chloride. We found that the reactions occurred on the sulfur atom keeping the C=C bond intact. The identity and properties of these complexes have been determined by spectroscopic methods and were compared to analogous systems. The X-ray crystal structure of **2** confirmed the atom connectivity of the Fe-Se-S-C=C moiety in which the alkene substituents are in a *trans* position.

Supplementary Information (SI)

Crystallographic data for the structural analyses of complex **2** have been deposited with the Cambridge Crystallographic Data Centre bearing the CCDC No. 2072989. Copies of this information are available on request free of charge from CCDC, Union Road, Cambridge, CB21EZ, UK (fax: +44-1223-336-033; e-mail: deposit@ccdc.ac.uk or <http://www.ccdc.cam.ac.uk>). All spectra of complexes **1** and **2** (Figures S1–S7) and full bond lengths and angles of **2** (Tables S1) are available at www.ias.ac.in/chemsci.

Acknowledgements

We thank the Deanship of Research, Jordan University of Science and Technology for financial support (Grant No. 243/2020).

References

- Braymer J J, Freibert S A, Rakwalska-Bange M and Lill R 2021 Mechanistic concepts of iron-sulfur protein

- biogenesis in biology *Biochim. Biophys. Acta, Mol. Cell Res.* **1886** 118863
- Jeong H S, Hong S, Yoo H S, Kim J, Kim Y, Yoon C, Lee S J and Kim S H 2021 EPR-derived structures of flavin radical and iron-sulfur clusters from Methylosinus sporium 5 reductase *Inorg. Chem. Front.* 1279
 - Nie X, Jäger A, Börner J and Klug G 2021 Interplay between formation of photosynthetic complexes and expression of genes for iron-sulfur cluster assembly in *Rhodobacter sphaeroides*? *Photosyn. Res.* **147** 39
 - Deane C 2020 An iron-sulfur grip *Nature Chem. Bio.* **16** 481
 - Buratto W R, Ferreira R B, Catalano V J, García-Serres R and Murray L J 2021 Cleavage of cluster iron-sulfide bonds in cyclophane-coordinated Fe_nS_m complexes *Dalton Trans.* **50** 816
 - Kertess L, Wittkamp F, Sommer C, Esselborn J, Rüdiger O, Reijerse E J, et al 2017 Chalcogenide substitution in the [2Fe] cluster of [FeFe]-hydrogenases conserves high enzymatic activity *Dalton Trans.* **46** 16947
 - Weigand W 2019 [FeFe]-hydrogenase mimics: Bio-inspired hydrogen production *Phosph. Sil. Sul. Rel. Elem.* **194** 634
 - Harb M K, Alshurafa H, El-khateeb M, Al-Zuheiri A, Görls H, Abul-Futouh H and Weigand W 2018 [FeFe]-hydrogenase models containing long diselenolato linkers *ChemSelect* **3** 8867
 - Abul-Futouh H, El-khateeb M, Görls H, Asali K J and Weigand W 2017 Selenium makes the difference: protonation of [FeFe]-hydrogenase mimics with diselenolato ligands *Dalton Trans.* **46** 2937
 - Wang H, Qiu X, Wang W, Jiang L and Liu H 2019 Iron sulfide nanoparticles embedded into a nitrogen and sulfur co-doped carbon sphere as a highly active oxygen reduction electrocatalyst *Front. Chem.* **7** 855
 - Wu X, Markir A, Xu Y, Hu E C, Dai K T, Zhang C, et al. 2019 Rechargeable iron-sulfur battery without polysulfide shuttling *Adv. Energy Mat.* **9** 1902422
 - Heift D 2019 Iron sulfide materials: catalysts for electrochemical hydrogen evolution *Inorganics* **7** 75
 - Vaccaro B J, Clarkson S M, Holden J F, Lee D-W, Wu C-H, Poole F L II, et al 2017 Biological iron-sulfur storage in a thioferrate-protein nanoparticle *Nature Comm.* **8** 16110
 - Maslat A, Jibril I, Abusaud M, Abed-Alhadi A and Hamadeh Z 2002 Synthesis and biological study of a new series of bifunctional organoiron thio- and selenoterephthalate derivatives $(C_5H_5)Fe(CO)_2ECO(C_6H_4)COX$ (E = S, X = R_2N , RNH , NH_2 , OH , Cl ; E = Se, X = RNH , RS , $RCOO$, NH_2 , OH , Cl) *Appl. Organomet. Chem.* **16** 44
 - Maslat A, Jibril I and Mizyed S 2010 Antimutagenic activities of two suspected anticarcinogenic bifunctional organoiron seleno-terephthalate derivatives *Drug Chem. Toxicol.* **33** 254
 - El-khateeb M, Al-Noaimi M, Al-Rejjal N, Abul-Futouh H, Görls H and Weigand W 2013 Mono- and bi-iron chalcogencarboxylate complexes *Trans. Met. Chem.* **38** 52917
 - Al-Jazzazi T, El-khateeb M, Quraan L, Abul-Futouh H, Görls H and Weigand W 2020 Half-sandwich iron complexes bearing vinyl-selenocarboxylato ligands *J. Chem. Sci.* **132** 23
 - El-khateeb M, Shaver A and Lebus A M 2001 The synthesis and structure of the thiosulfonato iron complexes $CpFe(CO)_2SS(O)_2R$ *J. Organomet. Chem.* **622** 293
 - El-khateeb M and Obidate T 2001 The first selenosulfonate complexes $CpFe(CO)_2SeSO_2R$: preparation and structure of $CpFe(CO)_2SeSO_2C_6H_5$ *Polyhedron* **20** 2393
 - El-khateeb M, Görls H and Weigand W 2007 *O*-Alkylthio- and *O*-alkylselenooxalate iron complexes: Structures of $CpFe(CO)_2ECOCO_2Me$ and $[CpFe(CO)_2ECO]_2$ *Inorg. Chim. Acta* **360** 705
 - El-khateeb M, Asali K J and Lataifeh A 2003 Half sandwich iron S-bonded mono-thiocarbonate complexes: structure of $CpFe(CO)_2SCO_2Et$ *Polyhedron* **22** 3105
 - El-khateeb M 2004 Iron Se-bonded mono-selenocarbonates $CpFe(CO)_2SeCO_2R$: the first selenocarbonate complexes *Inorg. Chim. Acta* **357** 4341
 - El-khateeb M, Asali K J and Lataifeh A 2006 Iron dithiocarbonate complexes: Structure of $CpFe(CO)_2SC(S)O-4-C_6H_4Cl$ *Polyhedron* **25** 1695
 - El-khateeb M 2006 Selenothiocarbonate complexes of iron: Structure of $CpFe(CO)_2SeC(S)O-4-C_6H_4Cl$ *Polyhedron* **25** 1386
 - El-khateeb M, Abul-Futouh H, Görls H, Weigand W and Almazahreh L R 2016 Synthesis, characterization and electrochemical investigations of heterocyclic-selenocarboxylate iron complexes *Inorg. Chim. Acta* **44** 14
 - El-khateeb M, Abul-Futouh H, Görls H and Weigand W 2019 Towards the synthesis of piano-stool iron complexes mediated by S-alkyl selenothiocarbonato ligands and their substitution reactions *Monatsh Chem.* **150** 1461
 - El-khateeb M and Roller A 2007 Synthesis and structures of $CpFe(CO)_2(\kappa E-ECS_2Ph)$ and $[CpFe(CO)(\kappa_2S, E-ECS_2Ph)]$ (E = S, Se) *Polyhedron* **26** 3920
 - Jibril I, El-Hinnawi M A and El-khateeb M 1991 Synthesis of a new series of iron complexes $Fe(C_5H_5)(CO)(EPh_3)SCOR$, $Fe(Bu^1-C_5H_4)(CO)(EPh_3)SCOR$ and $Fe(1,3-Bu^1-C_5H_3)(CO)(PPh_3)SCOR$ (E = P, As, Sb) through photolytic CO-substitution. Study of the effect of R, E and Cp-substituents on the CO-substitution reactions *Polyhedron* **10** 2095
 - El-khateeb M, Lataifeh A and Jibril I 2003 Substituted iron selenocarboxylate complexes $CpFe(CO)(EPh_3)SeCOR$ (E = P, As, Sb) *Trans. Met. Chem.* **28** 85
 - El-khateeb M, Kumar R and Yousuf S 2020 Halfsandwich iron S-alkyl dithiocarbonato complexes: Synthesis, characterization and reactivity *J. Mol. Struct.* **1211** 28092
 - El-khateeb M, Harb M K, Mansour A and Yousuf S 2019 Photochemical substitution of a single CO ligand of $CpFe(CO)_2SeC(Y)Y'Ar$ [(Y) $Y'=(O)$ O,(S) O and (S) S] by EPh_3 (E= P, As, Sb) *Inorg. Chim. Acta* **286** 694
 - Jibril I, El-khateeb M, Barakat H, Rheinwald G and Lang H 2002 Photolytic CO-substitution reaction of organoiron thiocarboxylate derivatives $CpFe(CO)_2SCOR$ (R=alkyl, aryl) with diphosphines $(Ph_2P(CH_2)_n$

- PPh₂) (n= 1–6): X-ray crystal structure of [CpFe(dppm)SCO(3,5-(NO₂)₂C₆H₃)] *Inorg. Chim. Acta* **333** 1
33. El-khateeb M, Jibril I, Barakat H, Rheinwald G and Lang H 2003 Controlled synthesis of mono-substituted diphosphine iron thiocarboxylate complexes CpFe(CO)(Ph₂P(CH₂)_nPPh₂)SCOR [n= 1 (dppm), n= 2 (dppe)]. X-ray crystal structure of CpFe(CO)(dppm-S)SCO-3,5-(NO₂)₂C₆H₃ *Polyhedron* **22** 3445
34. El-khateeb M, Asali K J, Al-Noaimi M, Al-Rabae E, Awwadi F, Taher D and Lang H 2014 Thio- and selenosulfonato complexes of iron bearing aromatic and heterocyclic groups *Inorg. Chim. Acta* **421** 553
35. El-khateeb M, Wolfsberger B and Schenk W A 2000 Sulfur (IV) compounds as ligands: Part XXV. Half-sandwich ruthenium thiosulfonato complexes. Crystal and molecular structure of [CpRu(dppe){SSO₂(4-C₆H₄Cl)}] *J. Organomet. Chem.* **612** 14
36. El-khateeb M, Görls H and Weigand W 2006 Half-sandwich ruthenium thiocarbonate complexes: Structures of CpRu(PPh₃)₂SCO₂Buⁿ, CpRu(dppe)SCO₂Buⁿ and CpRu(PPh₃)(CO)SCO₂Buⁿ *J. Organomet. Chem.* **691** 5816
37. El-khateeb M, Asali K J, Abu Salem T and Welter R 2006 Synthesis and characterization of cyclopentadienyltricarbonyl tungsten selenocarboxylate and selenosulfonato complexes *Inorg. Chim. Acta* **359** 4259
38. El-Hinnawi M A, Aruffo A A, Santersiero S, McAlister D and Schomaker V 1982 Organometallic sulfur complexes. 1. Syntheses, structures, and characterizations of organoiron sulfane complexes (μ-Sx)[(η⁵C₅H₅)]₂[Fe(CO)₂]₂ (x = 1–4) *Inorg. Chem.* **22** 1585
39. Herman W A, Rohrmann J and Hecht H 1985 Mehrfachbindungen zwischen hauptgruppenelementen und übergangsmetallen: XVII. Selen- und tellur-brücken in organometallkomplexen: AUFBAU, protonierung und methylierung *J. Organomet. Chem.* **290** 53
40. SAINT+, version 6.01: Area-Detector Integration Software, Bruker AXS, Madison 2001
41. Krause L, Herbst-Irmer R, Sheldrick G M and Stalke D 2015 SADABS 2016/02 *J. Appl. Crystallogr.* **48** 3
42. (a) Sheldrick G M 1990 Phase annealing in SHELX-90: direct methods for larger structures *Acta Crystallogr. A* **46** 467; (b) Sheldrick G M 2008 A short history of SHELX *Acta Crystallogr. A* **64** 112
43. Sheldrick G M 2015 Crystal structure refinement with SHELXL *Acta Crystallogr. C* **71** 3
44. Farrugia L J 2012 WinGX and ORTEP for windows: an update *J. Appl. Crystallogr.* **45** 849
45. El-khateeb M, Asali K J, Al-Junidi B, Abul-Futouh H, Görls H and Weigand W 2020 Synthesis, characterization and electrochemical investigations of heterocyclic-selenocarboxylate iron complexes *J. Chem. Sci.* **132** 22
46. Chand A, Sahoo D K, Rana Jena A S and Biswal H S 2020 The prodigious hydrogen bonds with sulfur and selenium in molecular assemblies, structural biology, and functional materials *Acc. Chem. Res.* **53** 1580
47. Senevirate D S, Uddin M J, Swarambunathan V, Schlegel H B and Endicott J F 2002 Characteristics and properties of metal-to-ligand charge-transfer excited states in 2,3-bis(2-pyridyl)pyrazine and 2,2'-bipyridine ruthenium complexes. Perturbation-theory-based correlations of optical absorption and emission parameters with electrochemistry and thermal kinetics and belated Ab Initio calculations *Inorg. Chem.* **41** 1502